Characterization and Application of Nanomaterials (2021) Volume 4 Issue 2
doi:10.24294/can.v4i2.1294

ORIGINAL RESEARCH ARTICLE

Template assisted nano-structured nickel for efficient methanol oxidation

S Mohanapriya*, V Raj

Advance Materials Research Lab, Department of Chemistry, Periyar University, Salem-636 011, India. E-mail: priyaechem@gmail.com

ABSTRACT

Nanoporous nickel has been prepared by electrodeposition using non-ionic surfactant based liquid crystalline template under optimized processing conditions. Physicochemical properties of nanoporous nickel are systematically characterized through XRD, SEM and AFM analyses. Comparison of electrocatalytic activity of nanoporous nickel with smooth nickel was interrogated using cyclic voltammetry (CV), chronoamperometry (CA) and electrochemical impedance spectroscopy (EIS) analyses. Distinctly enhanced electrocatalytic activity with improved surface poisoning resistance related to nanoporous nickel electrode towards methanol oxidation stems from unique nanoporous morphology. This nanoporous morphology with high surface to volume ratio is highly beneficial to promote active catalytic centers to offer readily accessible Pt catalytic sites for MOR, through facilitating mass and electron transports.

Keywords: Template Deposition; Electrocatalysis; Methanol Oxidation; Direct Methanol Fuel Cell

ARTICLE INFO

Received: 20 May 2021
Accepted: 11 July 2021
Available online: 18 July 2021

1. Introduction

Owing to the simplified system design, high energy density, and ease of transportation of fuel, direct methanol fuel cells (DMFCs) are currently at the forefront as renewable energy sources which involve electrochemical energy conversion and hence suitable for automotive as well as portable power applications[1–4]. Till now, Platinum (Pt) and its alloys represent the most extensively used DMFC electrocatalysts on account of their superior catalytic activity and stability towards oxidation of methanol at the anode side[5–7]. But the catalytic activity of the Pt surface could easily be deteriorated by the adsorption of CO generated during methanol oxidation reaction (MOR).

Promoting the effect of Ni over Pt catalytic activity both in acidic and alkaline mediums is well established in the literature[8–10]. Earlier studies established the role of nickel in assisting the dissociative adsorption of water molecules to produce-OH ads species, which facilitates the oxidation of CO adsorbed on Pt surface, thereby favors regeneration of Pt catalytic centers. Many electrodes involving nickel as a component in their manufacture can be used as catalysts in fuel cells. It is commonly used as an electrocatalyst for both anodic and cathodic reactions in organic synthesis and water electrolysis[15–18].

A very important application of nickel as a catalyst is the

oxidation of alcohol. Several studies on the electro-oxidation of alcohol on nickel have been reported. Alkaline direct methanol fuel cells are now receiving considerable attention because they allow the use of anion exchange membranes that reduce methanol cross-over—a serious problem with cation exchange membrane used in acidic methanol fuels[8]. Another reason for using an alkaline medium is because the kinetics for both methanol oxidation and oxygen reduction reactions is found to be more facile in an alkaline medium than in an acidic one[9–12]. In recent years, researchers focus on finding cheaper alternative electrocatalysts and improving the overall cell performance. Non-noble transition metal electrocatalysts such as copper[13–16], nickel[17–24], which oxidize methanol and other alcohols, offer good alternative electrocatalysts. The activity of nickel- based electrocatalysts depends on the method of preparation of these electrodes. Rahim *et al.*[24] showed that only nickel dispersed in graphite is catalytically active for methanol oxidation while massive nickel is not. In addition, this nickel electrocatalyst loses its performance due to the possible loss of nickel oxide activity after continuous circulation[24]. This is believed to be due to the increased thickness of NiO(OH), which acts as a barrier inhibiting the charge transfer process for methanol oxidation. Alternative approaches to prepare nickel electrocatalysts that can minimize the buildup of such a barrier layer would be of great interest in the development of non-noble metal electrodes for methanol oxidation. The purpose of the present work is to establish the electro-catalytic oxidation of methanol on Nanoporous nickel in a solution of 1.0 M NaOH. Surfactant mesophases come under the category of soft template systems and electrodeposition through them is a very useful and versatile method for the synthesis of nanostructured materials. In addition, lyotropic liquid crystalline phases possess a long-ranged spatially periodic architecture with lattice parameters in the range of a few nanometers. This makes them ideal candidate systems for the synthesis of nanomaterials. In this study, we report a simple electrochemical method of preparing a high surface area for nanoporous nickel deposit, using a new hexagonal liquid crystalline phase as a template. This room-temperature deposited nickel has been characterized by electrochemical techniques such as cyclic voltammetry (CV) and electrochemical impedance spectroscopy. Besides, scanning electron microscopy (SEM), atomic force microscopy (AFM), and X-ray diffraction (XRD) are also used for surface characterization. The catalytic efficiency of synthesized nanoporous nickel is evaluated by methanol oxidation using the techniques such as CV, Impedance, etc. And morphology and composition of nanoporous nickel cloud easily be tuned through controlling parameters involved in electrodeposition.

2. Materials and methods

2.1 Chemicals

Triton X-100 (Spectrochem), Polyacrylic acid (PAA) (Aldrich), sodium hydroxide pellets (Emerck), Ni(II) chloride (EMerck), nickel sulphamate (Grauer and Wheel), boric acid (Sarabhai chemicals) were used in this study. All chemical reagents used were AnalaR (AR) grade. Millipore water having a resistivity of 18 M cm was used in all the experiments.

2.2 Preparation and characterization of hexagonal liquid crystalline phase

The hexagonal liquid crystalline phase was prepared from a ternary mixture of Triton X-100, PAA, and water. We have carried out our studies at two different weight compositions viz., Triton X-100 + water (42/58 vol%). The mixture was stirred in a magnetic stirrer at a temperature of 33–35 ℃ for 1 h and cool down to room temperature. When viewed under a polarized light microscope, the mixture shows the characteristic birefringence of a hexagonal liquid crystalline phase-stable up to 29 ℃. All the electrodeposition using this phase as a template has been done at the room temperature of 25 ℃.

2.3 Nickel electroplating through hexagonal liquid crystalline

The electrodeposition of Nanoporous nickel was performed in a standard three-electrode glass cell using Al as a working electrode, a saturated calomel

electrode (SCE), and Pt foil served as a reference and counter electrodes respective. Nanoporous nickel synthesizes through electrodeposition at a constant of –1 V for a different periods. For electrodeposition, we have prepared the aqueous phase of the above described hexagonal liquid crystalline system from the standard nickel sulfamate bath[21] of the composition: 300 g/L nickel sulfamate, 6 g/L nickel chloride, and 30 g/L boric acids.

3. Results and discussion

3.1 Micro-structural analyses

Interesting electrocatalytic properties is exhibited by mesoporous nickel owing to their high surface area, unique morphology and high conductivity. Schematics of synthesis of steps involved in the process of preparation of Nanoporous nickel is illustrated in **Figure 1**. Triton X 100 forms micelles aggregated in the aqueous phase. Nickel ions encapsulated in the micelles of Triton X100 undergoes electrochemical reduction in such way that meso domains are created over the surface. Textural properties of nickel deposit are modified due to entrapment of nickel ions inside the micelles.

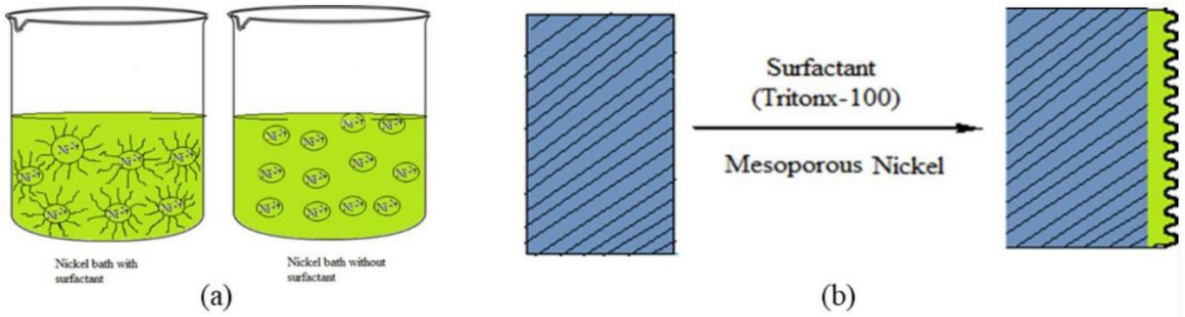

Figure 1. Preparation of the nanoporous nickel. **(a)** Pictorial representation of nickel bath with and without surfactant; **(b)** Schematic representation for preparation of Nanoporous nickel.

Nanoporous nickel was characterized by X-ray powder diffraction (XRD). XRD pattern of nickel deposited electrodes reveals the characteristic peaks expected for nickel with face-centered cubic (FCC) structure in addition to the reflections observed for bare Al electrode. Nanoporous nickel deposited show the peaks at 44.3° and 51.8° corresponding to (111) and (200) planes respectively and are indicated by the asterisk mark in the figure. The ratio of intensities of (111) and (200) planes associated with these nickel electrodes with and without surfactant suggests that there is a preferential growth and orientation of nickel film along (200) direction in the case of surfactant electro deposition. It can be noticed from the figure that the XRD pattern of nickel deposited electrodes reveals the characteristic peaks expected for nickel with a face-centered cubic structure.

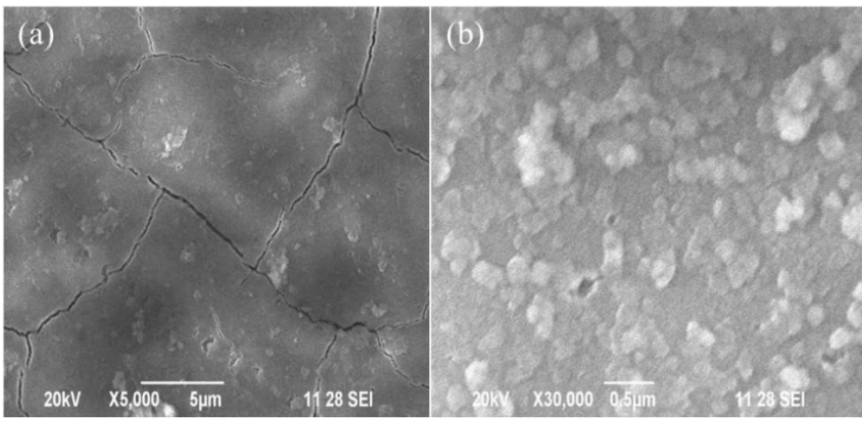

Figure 2. SEM images of **(a)** nanoporous nickel and **(b)** smooth nickel.

SEM pictures of nickel deposited on with and without the addition of Triton-X 100 are shown in **Figure 2**. The morphology of an individual deposit depends upon the electrolyte used for deposition. These images display the distinguishable structural features indicating the homogeneous growth of nickel deposits. Compared with nickel electrode produced without template, nickel deposited by template shows higher uniform growth.

The particles are same-sized spheres with smooth surfaces, the surface area can be related to the average equivalent particle size by $d = 6000/(\rho.s)$ (in nm), where d is the average diameter of spherical particle in manometer; ρ is the theoretical density of nickel (g/cm^3) and s represents the measured surface area of the powder in m^2/g. The size of the particles is in the range of 5–10 μm. Compared to the both images, nanoporous nickel surface morphologies present higher roughness.

AFM studies also validate the above observation as presented by **Figure 3**. AFM studies are used to demonstrate the difference in topography of nanoporous nickel and smooth nickel. Difference in the surface topographies related to nanoporous nickel and smooth nickel are evaluated through AFM analysis. Nanoporous structure helps to improve electronic conductivity which is highly advantageous for efficient electrocatalysis. The modulations in the height profile indicate that synthesized nanoporous nickel is associated with high degree of roughness. Surface modulations on the nanoporous nickel drastically increase the roughness factor associated with it, however nickel deposited using electrolyte bath without addition of surfactant exhibits two times lower roughness.

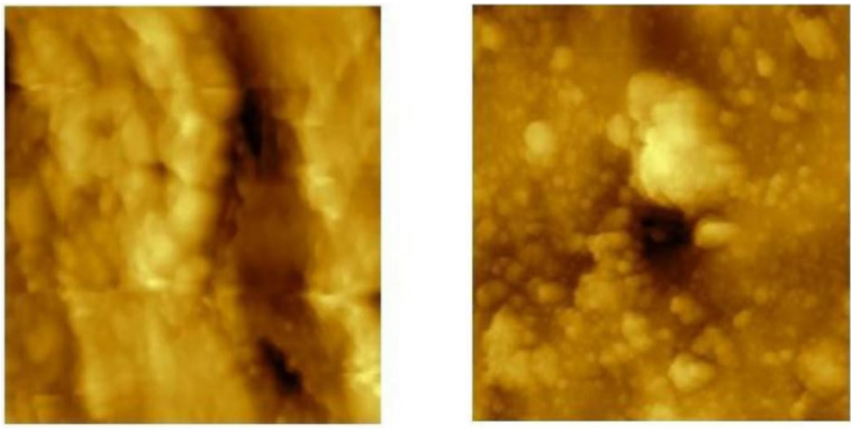

Figure 3. AFM images of smooth nickel and Nanoporous nickel.

It is because that this unique porous structure electrocatalytic activity of nanoporous nickel is higher. Distinct porous structure of nanoporous deposits substantially increases the surface area. SEM and XRD studies are in good agreement with AFM results.

3.2 Electrochemical studies

The electrochemical activity of mesoporous nickel electrode was studied by cyclic voltammetry, amperometry and electrochemical impedance techniques. The cyclic voltammograms (CV) of nickel deposited with and without the addition of Triton-X100 were recorded in alkaline medium. The CV measurements were conducted in 0.1 M NaOH at scanning rate of 100 mV/s. The applied potential was limited between 1 and –1 V.

When discussing the electrochemical behavior of nickel, it is convenient to consider the three oxide phases formed when a positive potential is applied to the metallic nickel electrode. A cyclic voltammetry (CV) profile of nickel in aqueous alkaline solution reveals features corresponding to the formation of three oxide species as the potential increased from –1 to 1 V vs hydrogen evolution reaction. The an-

odic peak corresponding to the formation of the first surface oxide, α-$Ni(OH)_2$, is present in the V range of –1 to 1 V. If the CV scan is reversed at a potential lower than 0.50 V, the full reduction of α-$Ni(OH)_2$ to metallic nickel will occur, giving rise to a cathodic peak in the CV profile at $-1 \leq E \leq 1$ V. When the potential is brought to values lower than 0 V, appreciable current density as a result of the hydrogen evolution reaction (HER) is observed along with the formation of H_2 (gas) bubbles at the electrode. The HER overlaps in potential with the reduction of α-$Ni(OH)_2$.

If the forward CV scan continues to have potentials higher than 0.50 V, the α- $Ni(OH)_2$ already present on the electrode converts to β-$Ni(OH)_2$, and an additional β-$Ni(OH)_2$ is formed. This species forms in the E region between 0.50 V and 1.30 V, which is known as the passive potential region for a nickel. Of these two $Ni(OH)_2$ structures, the β phase is more stable. The formation of this phase is irreversible, meaning that β-$Ni(OH)_2$ cannot be removed from the surface of the electrode by simply reversing the potential and reducing the oxide electrochemically. Once formed, β-$Ni(OH)_2$ can be removed through chemical etching, mechanical polishing, and thermal reduction in a hydrogen environment. The α- and β-$Ni(OH)_2$ species have different crystallographic structures; the α phase incorporates either water or alkali cations from the electrolyte and has a lattice constant that is larger than that of β-$Ni(OH)_2$. The final oxidation species to be formed is NiOOH. At $E >$ 1.30 V, the β-$Ni(OH)_2$ species is oxidized reversibly to β-NiOOH, which has a similar crystallographic structure and lattice constant. If an increasing positive potential is continuously applied, a γ-NiOOH phase is formed. This species adopts a crystallographic structure similar to that of α-$Ni(OH)_2$ and can be electrochemically reduced back to β-$Ni(OH)_2$.

From **Figure 4a**, it is evident that nanoporous nickel deposits present a higher current density compared to smooth nickel prepared without the addition of surfactant. It reports that periodic nanoporous structures with a high surface area can have charge storage capacity by one order over that of the bulk materials. Increased electrochemical surface area of nanoporous deposits are due to the presence of Triton-X100 molecules during a deposition process. These surfactant molecules act as a template during deposition, create mesopores in the nickel surface, and favor the formation of highly active nanoporous nickel deposits. Owing to the larger surface area, electrochemically active surface area is also higher for the nanoporous nickel deposits.

Higher roughness associated with mesopores nickel is due to the larger number of electrolytes accessing channels formed over nanoporous nickel due to more availability of electrolyte access-electrochemical surface area. In other words, through the nanoporous deposits, electrolytes could easily reach the nickel surface compared to smooth nickel.

The electrocatalytic response of prepared nickel deposits is evaluated through the addition of 1 M methanol. CV curves of nickel deposits before and after the addition of 1 M methanol in 0.1 M aqueous

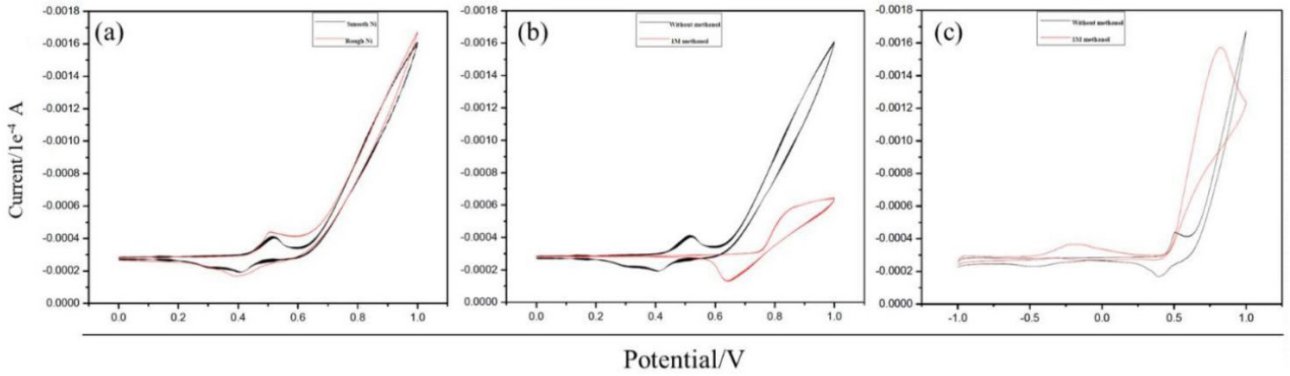

Figure 4. Cyclic voltammetric curves of different nickel materials scanned from –1 to 1V at a rate of 50 mV/s in 0.1 M NaOH. **(a)** Nanoporous nickel and smooth nickel; **(b)** smooth nickel with and without 1M methanol, and **(c)** nanoporous nickel with and without 1 M methanol.

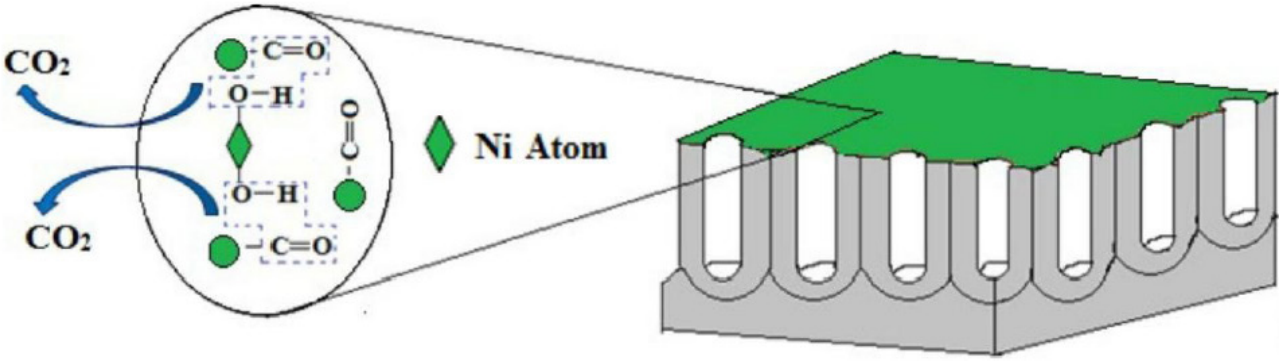

Figure 5. Mechanism of electro-oxidation of methanol on nanoporous nickel catalyst.

NaOH solution are given in **Figure 4b** and **Figure 4c** correspondingly. Since NiOOH was constantly being reduced back to $Ni(OH)_2$, once methanol oxidation started, some anodic current could always be attributed to the continuous re-oxidation of $Ni(OH)_2$ back to NiOOH. Furthermore, during the cathodic scans, lingering methanol oxidation caused some portion of the electrode surface to be prematurely reduced to the Ni(II) oxidation state before the Ni(III)/Ni(II) reduction occurred, thus decreasing the amount of NiOOH on the surface and the magnitude of the corresponding peak. By comparing the electrocatalytic response of methanol on nanoporous nickel and smooth nickel, it is clear that the anodic peak current associated with methanol electro-oxidation is higher for nanoporous nickel. An increase in the anodic peak current on the addition of 1 M methanol is 0.0012 and 0.0002 mA/cm^2 for nanoporous nickel and smooth nickel respectively. The improved current response demonstrates the significance of nanoporous structure.

The onset of methanol oxidation occurs at about 500 mV at the nanoporous nickel electrode whereas methanol oxidation begins from 550 mV with a smooth nickel electrode. A lower onset potential associated with nanoporous nickel evidences higher electrocatalytic activity for MOR. The superior catalytic activity of nanoporous nickel may stem from unique porous morphology associated with higher ESCA. It is evident that the peak potential at which methanol oxidation occurs on nanoporous nickel is 0.75 V, but 0.85 V for a smooth nickel.

As well known, the forward current peak (*If*) is attributed to the oxidation of methanol molecule and the backward current peak (*Ib*) to the oxidation of adsorbed intermediates such as CO, CH_xOH ($0 < x < 2$), CH_xO, HCOO- and so on. Hence, the number of oxidizable intermediates adsorbed over the catalytic surface could be predicted by the relative magnitude of backward peak. (*If*)/(*Ib*) ratio is a measure of the efficiency of a catalyst to tolerate the poisoning of the surface due to adsorption of incompletely oxidized intermediates. (*If*)/(*Ib*) value for nanoporous nickel and smooth nickel is 1.3 and 1.17 respectively, which are higher than that of pure Pt as reported earlier. A higher (*If*)/(*Ib*) value indicates that most of the intermediate carbonaceous species were oxidized to carbon dioxide in the forward scan on the nanoporous nickel electrode. Increased CO tolerance of nanoporous nickel electrode may be attributed due to the basic difference in methanol oxidation between nanoporous and nonporous structure, which could be explained on the basis of morphology-dependent CO tolerance as demonstrated earlier.

Based on the results, it could be inferred that nanoporous architecture increases poisoning tolerance of the catalyst through influencing the availability of continuous binding sites for C-H bond cleavage and enhances a greater number of readily accessible active catalytic sites for methanol oxidation reaction (MOR). The schematic illustration of the mechanism of CO removal over nanoporous nickel is depicted in **Figure 5**.

Various concentrations of methanol 2 M, 3 M, 4 M, and 5 M were added to smooth nickel and nanoporous nickel. Smooth nickel has good electrocatalytic activity, but surfactant tritonx-100 nickel has high electrocatalytic activity shown in **Figures**

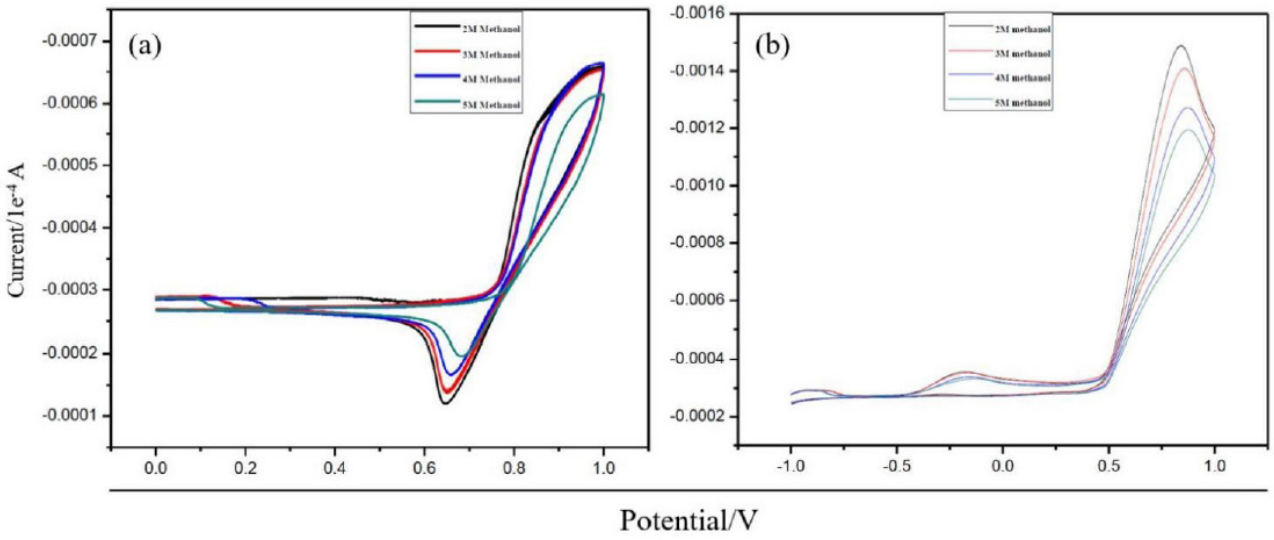

Figure 6. Cyclic voltametric curves of **(a)** smooth nickel and **(b)** nanoporous nickel in various concentration of methanol scanned from –1 to 1V at a rate of 50 mV/s performed in 0.1 M NaOH.

6a and **6b** respectively.

CV curves were used to examine the electrochemical properties of nanoporous nickel in an aqueous alkaline electrolyte and to relate such acquired insight to their chemical composition and surface characteristics. Typical CV curves for bulk nickel in aqueous NaOH solution in the –1 to +1 V potential (E) range show the following anodic features:

i. Oxidation of metallic nickel to α-$Ni(OH)_2$ at $0.20 < E < 0.40$ V;

ii. Concurrent conversion of α- to β-$Ni(OH)_2$ and oxidation of metallic nickel to β-$Ni(OH)_2$ at $0.50 < E < 1.30$ V;

iii. The oxidation state of Ni Increases from +2 to +3 through the oxidation of β-$Ni(OH)_2$ to β-NiOOH at $1.30 < E < 1.55$ V;

iv. Oxygen evolution reaction (OER) at $E \geq 1.55$ V.

The β phase of $Ni(OH)_2$ is the most stable and thermodynamically favored oxide of nickel; it is the passive layer that develops on the surface of metallic nickel upon contact with the ambient environment. The conversion of α- to β-$Ni(OH)_2$ is irreversible, and once it takes place, the cathodic peak corresponding to the reduction of α-$Ni(OH)_2$ is not observable anymore. The reduction of β-$Ni(OH)_2$ cannot be accomplished electrochemically and can be achieved at elevated temperatures in the presence of H_2 (g). The anodic and cathodic peaks characteristic of α-$Ni(OH)_2$ formation and reduction are not observed because a layer of β-$Ni(OH)_2$ has developed as the result of several prior CV scans. The CV curves for nickel nanoporous display the same features as those observed for smooth nickel in alkaline media. The CV curves for nanoporous nickel reveal pronounced differences, especially in the anodic scan. Compared to the mesoporous nickel, the peak is shifted towards higher potentials and overlaps the region of OER. The value of I_s for OER is greater than that of nickel nanoporous; the specific current for the cathodic feature is greater than that of nickel nanoporous, but the difference is small. Nickel and nanoporous nickel have very different surface morphologies, and the rough, bubbly surface of nanoporous nickel gives rise to a larger surface area than a smooth nickel. The charges under the two cathodic peaks are similar, thus indicating that both samples have similar amounts of β-NiOOH on the surface. The difference in Q_s values for smooth nickel is less than 40%, and that nanoporous nickel has a significantly larger actual surface area, we conclude that β-NiOOH does not make up the entire surface of nanoporous nickel.

3.3 Chronoamperometry

To evaluate the long-term activity of the catalyst, the steady-state current responses of nanoporous nickel and smooth nickel were recorded (**Figure 7**).

Initial rapid current decay for both catalysts is due to double-layer capacitance. Transient current due to methanol oxidation attains a steady state after 820 s and 1600 s with nanoporous nickel electrode and smooth nickel electrode respectively, indicating the better catalytic performance of the former. It could be noticed from chronoamperometric results that the addition of 1 M methanol shows an increased electrocatalytic response on nanoporous nickel surface but the increased current response is not very high with smooth nickel. As evident from the figures, the addition of 1 M methanol causes an increase in current 0.07 A/cm^2 for nanoporous nickel and 0.0001 mA/cm^2 for smooth nickel.

Methanol oxidation current tends to decrease due to the accumulation of adsorbed species on catalyst surfaces due to the decomposition of methanol molecules. By comparing the current responses, it is obvious that the nanoporous nickel electrode possesses enhanced catalytic durability. Unique nanoporous structure comprising continuous Meso channels is highly favorable to provide easy transport paths of electrons and reaction intermediates, therefore, enhances MOR activity of nanoporous nickel electrode.

3.4 Impedance studies

To further extract information about the electro catalytic process, EIS studies are performed. **Figures 8a** and **8b** represent Nyquist plots recorded at 500 mV dc-offset potential in 0.1 M NaOH with methanol for nanoporous nickel and smooth nickel electrodes respectively.

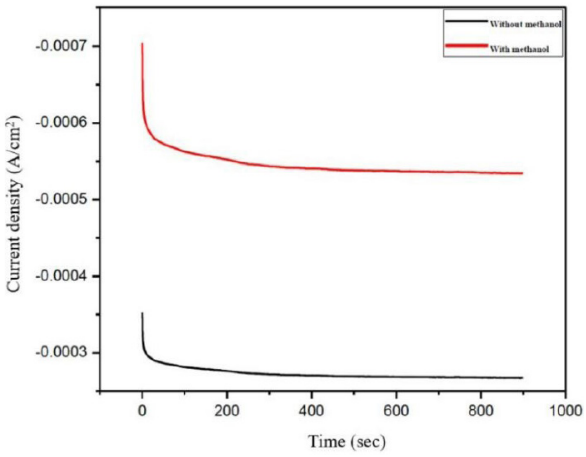

Figure 7. Amperometric curves of Nanoporous nickel with and without 1 M methanol.

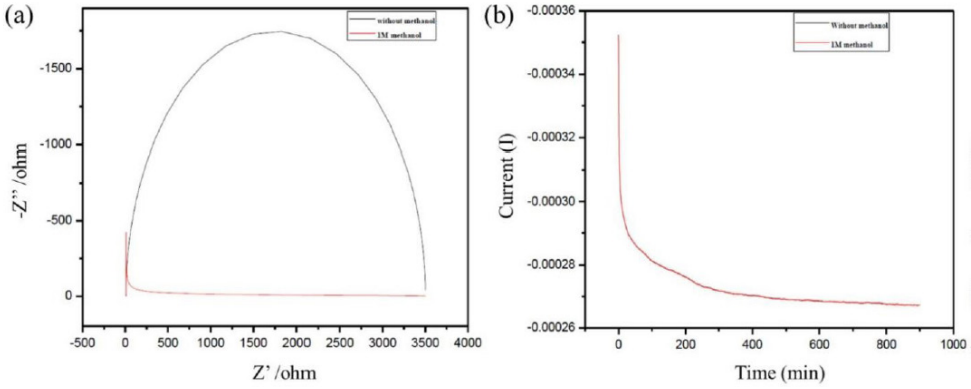

Figure 8. Impedance of **(a)** Nanoporous nickel and **(b)** smooth nickel deposition, with or without 1 M methanol.

General pattern of Nyquist plot obtained with electrodes under study is unaltered on changing the concentration of methanol from 0.1 to 4 M, pointing that mechanism of methanol oxidation is not affected by methanol concentration. Conversely, diameter of semicircle has been dramatically decreased on increasing the concentration of methanol, denoting that charge transfer resistance (Rct) regularly drops.

EIS analysis was carried out by fitting the data with appropriate equivalent circuit as shown in **Table 1**. Equivalent circuit is composed of solution resistance (R_s), double layer capacitance (CPE_1) and charge transfer resistance (R_{ct}) associated with MOR. Porous nature of electrode is attributed by the presence of additional elements namely CPE_2 and R_f. The values for all the parameters R_{ct}, CPE_1, CPE_2, and their associated % error determined by the fitting of the experimental EIS data are summarized in **Table 1**.

Table 1. Numerical values of elements in the equivalent circuit fitted with Nyquist plots of nanoporous and smooth nickel

Type	R_s (Ω)	CPE_1 ($\times 10^6$ ΩS^n)	n_1	R_{ct} (Ω)	CPE_2 ($\times 10^6$ ΩS^n)	n_2	R_f (Ω)	[Methanol] (mol/L)
Nanoporous nickel	14.80	4.186	0.91	1866.7	9.930	0.92	32380	0
	12.78	5.636	0.87	875.5	7.950	0.94	632.7	1
	11.65	6.100	0.88	153.3	4.280	0.91	449.7	2
	11.50	2.680	0.92	102.2	2.998	0.93	427.2	3
	11.58	4.220	0.96	82.2	1.746	0.89	499.1	4
Smooth nickel	15.10	5.767	0.88	3381.9	2.500	0.89	89342	0
	15.02	3.761	0.89	1505.0	4.536	0.90	6861.4	1
	12.50	2.504	0.85	771.4	3.089	0.91	739.5	2
	12.30	5.766	0.91	537.8	5.292	0.89	324.8	3
	12.32	4.340	0.89	331.7	4.700	0.95	241.9	4

The parallel combination of the charge-transfer resistance (R_{ct}) and CPE take into account for methanol adsorption and oxidation on porous thin film.

From **Figure 8a**, it can be seen that the R_{ct} values are found to decrease in the order 1 M methanol > without methanol. Without methanol is low resistance compared to 1 M methanol. The diameter of the semicircle is proportional to the value of the impedance. The smaller the value of impedance, the better the conducting property of the coating will be. This can be further confirmed by its low resistance and high capacitance.

Likewise, the equivalent circuit shown **Figure 8b** is a simplified electrochemical model, which has been used to fit the impedance data obtained for the composite coatings present on substrate. As can be seen from the equivalent circuit, R_s refers to the resistance of the solution, C_{dl} is the electric double layer capacitance and R_{ct} is the charge transfer resistance that represents the electrochemical activity of the electrode. Based on equivalent circuit model proposed, these EIS curves were best fitted. Various concentration of methanol solution in Tritonx-100 surfactant of the deposited nickel has low resistance and high capacitance.

The parallel combination R_{ct} with CPE leads to a depressed semicircle in the corresponding Nyquist impedance plot. It is noteworthy that R_{ct} is an order lower for nanoporous nickel than that of smooth nickel, which reflects the enhanced electrocatalytic activity of the former (**Figure 9**). The electrochemical impedance spectroscopic (EIS) is a power tool for studying the electrochemical behavior of electrode.

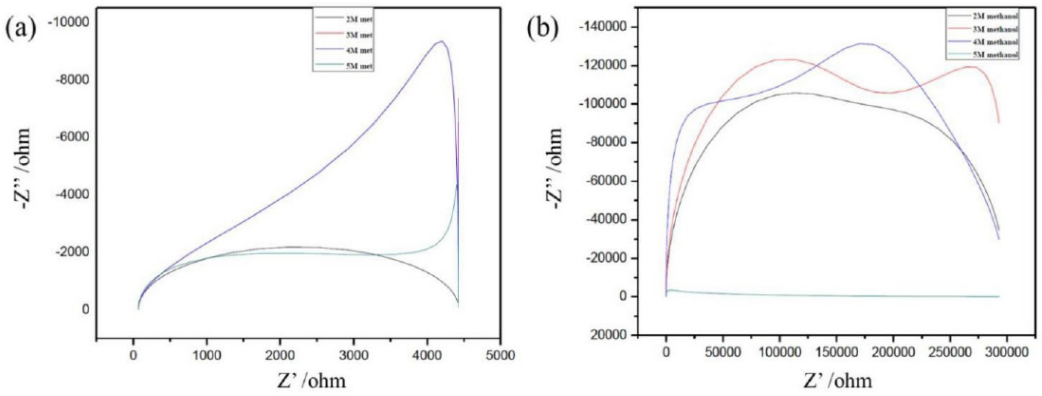

Figure 9. Impedance of **(a)** nanoporous and **(b)** smooth nickel deposition at 2, 3, 4 and 5 M methanol.

4. Conclusions

In a nutshell, a facile and simple approach to produce nanoporous nickel through electrode-position is by using surfactant Triton-X100. The developed methods are scalable and reproducible Triton-X100 template could be easily removed by washing the electrode with water. Nanoporous nickel has been prepared by surfactant assistant assisted electrochemical deposition of nickel under optimized process conditions. Surface characteristics of the nanoporous nickel and smooth nickel were systematically characterized through XRD, SEM, and AFM analyses. Nanoporous morphology is highly beneficial to offer readily accessible catalytic sites for methanol oxidation reaction (MOR), through facilitating mass and electron transport. The prepared nickel was used as electrocatalyst for DMFC. Comparison of electrolytic activity of nanoporous nickel with smooth nickel was interrogated using cyclic voltammetry (CV), chronoamperometry (CA) and electrochemical impedance spectroscopy (EIS) analyses. Distinctly enhanced electrocatalytic activity with improved CO tolerance associate with nanoporous nickel electrode towards methanol oxidation stems from readily accessible high surface area associated with nanoporous structured, which facilitate mass transport of both the reactants and products.

Conflict of interest

No conflict of interest was reported by the authors.

Acknowledgements

One of the authors S. Mohanapriya is grateful to University Grants Commission (UGC), Government of India, for providing fund under the scheme of "UGC-Dr. D. S. Kothari Post-Doctoral Fellowship". (Ref: No. Award Letter No.F.4-2/2006 (BSR)/CH/14-15/0102 dated 5-5-2015).

References

1. Liu H, Song C, Zhang L, *et al.* A review of anode catalysis in the direct methanol fuel cell. Journal of Power Sources 2006; 155(2): 95–110.
2. Neburchilov V, Martin J, Wang H, *et al.* A review of polymer electrolyte membranes for direct methanol fuel cells. Journal of Power Sources 2007; 169(2): 221–238.
3. Mohanapriya S, Bhat SD, Sahu AK, *et al.* A new mixed-matrix membrane for DMFCs. Energy & Environmental Science 2009; 2(11): 1210–1216.
4. Mohanapriya S, Bhat SD, Sahu AK, *et al.* Sodium-alginate-based proton-exchange membranes as electrolytes for DMFCs. Energy & Environmental Science 2010; 3(11): 1746–1756.
5. Mohanapriya S, Sahu AK, Bhat SD, *et al.* Bio-composite membrane electrolytes for direct methanol fuel cells. Journal of the Electrochemical Society 2011; 158(11): B1319–B1328.
6. Mohanapriya S, Bhat SD, Sahu AK, *et al.* Modified-bio-polymeric-mixed-matrix-membrane electrolytes for direct methanol fuel cells. Journal of Bionanoscience 2009; 3(2): 131–138.
7. Suganthi S, Mohanapriya S, Raj V. Biocomposite proton-exchange membrane electrolytes for direct methanol fuel cells. Journal of Applied Polymer Science 2016; 133(25): 43514.
8. Iwasita T. Electrocatalysis of methanol oxidation. Electrochimica Acta 2002; 47: 3663–3674.
9. Radmilovic V, Gasteiger HA, Ross PN. Structure and chemical composition of a supported Pt-Ru electrocatalyst for methanol oxidation. Journal of Catalysis 1995; 154(1): 98–106.
10. Antolini E, Salgado J, Gonzalez ER. The methanol oxidation reaction on platinum alloys with the first row transition metals: The case of Pt–Co and –Ni alloy electrocatalysts for DMFCs: A short review. Applied Catalysis B Environmental 2006; 63(1-2): 137–149.
11. Wasmus S, Kuver A. Methanol oxidation and direct methanol fuel cells: A selective review. Journal of Electroanalytical Chemistry 1999; 461(1-2): 14–31.
12. Iwasita T, Hoster H, John-Anacker A, *et al.* Methanol oxidation on PtRu electrodes. Influence of surface structure and Pt-Ru atom distribution. Langmuir 2000; 16(2): 522–529.
13. Wang K, Gasteiger HA, Markovic NM, *et al.* On the

reaction pathway for methanol and carbon monoxide electrooxidation on Pt-Sn alloy versus Pt-Ru alloy surfaces. Electrochimica Acta 1996; 41(16): 2587–2593.

14. Hu Y, Zhang H, Wu P, *et al.* Bimetallic Pt-Au nanocatalysts electrochemically deposited on graphene and their electrocatalytic characteristics towards oxygen reduction and methanol oxidation. Physical Chemistry Chemical Physics Cambridge Royal Society of Chemistry 2011; 13: 4083–4094.
15. Liu X, Cui C, Gong M, *et al.* Pt–Ni alloyed nanocrystals with controlled architectures for enhanced methanol oxidation. Chemical Communications 2013; 49: 8704–8706.
16. Xu D, Liu Z, Yang H. Solution-based evolution and enhanced methanol oxidation activity of monodisperse platinum-copper nanocubes. Angewandte Chemie International Edition 2009; 48(23): 4217–4221.
17. Mohanapriya S, Suganthi S, Raj V. Mesoporous Pt–Ni catalyst and their electro catalytic activity towards methanol oxidation. Journal of Porous Materials 2017; 24(2): 355–365.
18. Abdel Rahim MA, Hassan HB, Abdel Ham RM. Graphite electrodes modified with platinum-nickel nano-particles for methanol oxidation. Fuel cells 2007; 7(4): 298–305
19. Niu Z, Wang D, Yu R, *et al.* Highly branched Pt–Ni nanocrystals enclosed by stepped surface for methanol oxidation. Chemical Science 2012; 3(6): 1925–1929.
20. Ganesh V, Lakshminarayanan V. Preparation of high surface area nickel electrodeposit using a liquid crystal template technique. Electrochimica Acta 2004; 49(21): 3561–3572.
21. Xia Y, Xiong Y, Lim B, *et al.* Shape-controlled synthesis of metal nanocrystals: Simple chemistry meets complex physics? Angewandte Chemie International Edition 2009; 48(1): 60–103.
22. Mohanapriya S, Tintula KK, Bhat SD, *et al.* A novel multi-walled carbon nanotube (MWNT)-based nanocomposite for PEFC electrodes. Bulletin of Materials Science 2012; 35(3): 297–303.
23. Julia van D, Brandy Kinkead P, Yoseif M, *et al.* Electrochemically active nickel foams as support materials for nanoscopic platinum electrocatalysts. ACS Applied Materials & Interfaces 2014; 6(15): 1–73.
24. Mohanapriya S, Suganthi S, Raj V. Mesoporous Pt–Ni catalyst and their electro catalytic activity towards methanol oxidation. Journal of Porous Materials 2017; 24(2): 355–365.
25. Xing W, Li F, Yan Z, *et al.* Synthesis and electrochemical properties of mesoporous nickel oxide. Journal of Power Sources 2004; 134(2): 324–330.
26. Skowronski JM, Wazny A. Nickel foam-based $Ni(OH)_2$/NiOOH electrode as catalytic system for methanol oxidation in alkaline solution. Journal of New Materials for Electrochemical Systems 2006; 9(4): 345–351.
27. Rahim M, Hameed R, Khalil MW. Nickel as a catalyst for the electro-oxidation of methanol in alkaline medium. Journal of Power Sources 2004; 134(2): 160–169.